Catalysis Today 141 (2009) 288–293

Contents lists available at ScienceDirect

Catalysis Today

journal homepage: www.elsevier.com/locate/cattod

# MoV-based catalysts in ethane oxidation to acetic acid: Influence of additives on redox chemistry

M. Roussel [a], S. Barama [a], A. Löfberg [a], S. Al-Sayari [b], K. Karim [b], E. Bordes-Richard [a,*]

[a] Unité de Catalyse et de Chimie du Solide,UMR-CNRS 8181, ENSCL-USTL, Villeneuve d'Ascq, France
[b] SABIC R&T, P.O. Box 42503, Riyadh, Saudi Arabia

ARTICLE INFO

*Article history:*
Available online 22 July 2008

*Keywords:*
MoVO-based catalysts
Influence of Nb
Influence of palladium
Ethane oxidation
Acetic acid

ABSTRACT

The formation of acetic acid and/or ethylene by oxidation of ethane is strongly dependent on X additives or Y promotor added to MoVO-based catalysts. $MoV_{0.4}X_{0.12}Y_{\varepsilon}O_z$ (X = Nb; Y = Pd; $\varepsilon = 10^{-4}$) catalysts were prepared by the slurry method and their structural properties were studied by in situ (redox conditions) XRD, Raman and XPS techniques. The reactivity during reduction and reoxidation was analysed by thermal analysis (TGA/DSC). The oxidation of ethane was carried out in a conventional fixed bed microreactor with on line analysis by gas chromatography. Results show that Nb exerts mainly a structural effect as it is responsible for the stabilisation of molybdenum (VI) by formation of solid solutions with V, and that Pd modifies the rate of reduction of the solid catalysts. The increase of selectivity to acetic acid observed by Pd promotion is likely due to the transformation of ethylene to acetic acid occurring on neighboring Pd–V active sites.



## 1. Introduction

Considerable progress has been made to master the mild oxidation of $C_1$–$C_4$ alkanes towards valuable chemicals, except in the case of the oxidative dehydrogenation to alkenes [1,2]. As it comes out from literature, the combination of vanadium and molybdenum MoV oxides gives rise to catalysts able to transform benzene to maleic anhydride, acrolein or propane to acrylic acid, propane to acrylonitrile, and ethane to acetic acid and/or ethylene. The latter process has recently been commercialised by Sabic [3,4]. The fact that various reactant molecules can be oxidized to different products on the same type of catalyst is very unusual in mild oxidation [5,6]. The adaptation of MoV oxides to one or the other reaction is an intrinsic property of this system which is versatile enough to incorporate additives and promotors. Whatever their nature and their content, these additives are responsible for the stabilisation of certain crystal structures. They influence as well the behaviour of the main redox couple (e.g., $Mo^{6+}/Mo^{5+}$) in operating conditions, that is when the redox power of the catalytic solid faces the redox power of reactants (steam and/or oxygen, and alkane).

The oxidation of ethane to acetic acid on MoVNbO system has been pioneered by Thorsteinson et al. [7], and other catalysts based on vanadium oxide or on polyoxometallates supported on $TiO_2$ [8–10] or $ZrO_2$ [11], have also been studied. MoVNbO catalysts have been investigated as thoroughly as the MoV basis provides efficient catalytic formulae for the (amm)oxidation of propane. The discovery of the – now universally called – M1 (orthorhombic) and M2 (hexagonal) phases for the latter reaction gave rise to a day after day increasing literature, so that only a few authors are quoted here [12–19]. Restricting ourselves to the MoVNbO system for the oxidation of ethane to acetic acid, other stoichiometries were studied, as, e.g., $Mo_6V_3Nb_1$ by Burch and Swarnakar [20]. The method of preparation of the optimum formula $Mo_{0.73}V_{0.18}Nb_{0.9}O_y$ proposed by Thorsteinson et al. [7] was examined by Merzouki et al. [21,22]. They found that the formation of acetic acid or ethylene was observed when $Mo_5O_{14}$ or $Mo_{18}O_{52}$ respectively was identified by XRD, V and/or Nb being possibly included in these suboxides as solid solutions [23]. The properties of this MoVNbO system, including when it is modified by promotors, have recently been studied, mainly for the oxidative dehydrogenation of ethane (ODH) [24,25], in which cases the formation of $V_9Mo_6O_{40}$ is generally observed. When studied for the production of acetic acid which proceeds at lower temperature than ODH [26–28], the $Mo_5O_{14}$-type oxide is generally identified by X-ray diffraction (XRD) and Raman spectroscopy [29–32], and its presence may be a key factor to relate with the catalytic properties [21,22]. However, even though a same phase (e.g., $Mo_5O_{14}$) would be present, the influence of dopants or additives like W vs. Mo, Nb, and Al vs. Te or Sb, etc., is prominent owing to their different cationic Lewis-type

* Corresponding author. Tel.: +33 3204 34526; fax: +33 3204 36561.
*E-mail address:* Elisabeth.Bordes@univ-lille1.fr (E. Bordes-Richard).

0920-5861/$ – see front matter © 2008 Elsevier B.V. All rights reserved.
doi:10.1016/j.cattod.2008.04.046

acidity and to the possible implication of complementary redox systems [33,34].

Some structural and catalytic properties of $Mo_1V_{0.4}Nb_{0.12}Pd_\varepsilon O_z$ varying by the presence or absence of Pd dopant and/or Nb additive in the oxidation of ethane to acetic acid have already been studied [35,36], and the main results will be first recalled before exposing those obtained by redox experiments carried out by in situ methods.

## 2. Experimental

Catalysts $MoV_{0.4}Nb_{0.12}Pd_\varepsilon O_z$ ($\varepsilon = 10^{-4}$) were prepared by the slurry method according to patents [3,4], using ammonium salts of Mo and V, Pd chloride and/or Nb oxalate. The solid precursors were obtained after filtration of slurry and drying (110 °C, 8 h), and were first calcined up to 250 °C in air (3 h) before heat treatment in Ar up to 350 °C (3 h). Samples $MoV_{0.4}$, $MoV_{0.4}Pd_\varepsilon$, $MoV_{0.4}Nb_{0.12}$ and $MoV_{0.4}Nb_{0.12}Pd_\varepsilon$ are respectively called MoV, MoVPd, MoVNb, MoVNbPd further in the text.

The solids were studied by X-ray diffraction (Huber D5000, CuKα radiation) and in situ HT-XRD (Siemens D5000 diffractometer equipped with a HTK 1200 Anton Paar device and PSD detector, CuKα radiation). Samples were heated at 0.06 °C/s in HC/$N_2$ = 20/80 (HC = $H_2$, $C_3H_8$ or $C_2H_6$) and patterns were registered at 300, 350, 400 and 450 °C (30 min at each temperature). After cooling down and sweeping by $N_2$, the sample was reoxidized in $O_2/N_2$ = 20/80, and then it returned back to room temperature (R.T.) in the same atmosphere. The laser (micro)Raman spectroscopy (LRS) was carried out on Labram Infinity laser Raman spectrometer (JY-DILOR®). The reactivity of samples was qualitatively examined by submitting powder particles to the laser beam and decreasing the intensity of filter (D3: 0.04, D2: 0.05, D1: 0.08, D0.6: 0.48 and D0: 0.67 mW). In situ LRS was performed in different (reducing or oxidizing) atmospheres. Pure $H_2$ was chosen to simulate strong local reducing atmosphere as it can occur during catalysis, and synthetic air (20/80 $O_2/N_2$) as an oxidizing atmosphere. X-ray photoelectron spectroscopy (XPS) was performed on ESCALAB 220XL spectrometer. The AlKα monochromatized line (1486.6 eV) was used at 120 kV (500 μm spot diameter). The powder samples were pressed in a 2 mm hole on a steel block. The spectrometer was operated in a constant pass energy mode ($E_{pass}$ = 30 eV) at a pressure less than $10^{-7}$ Pa. Experimental quantification level and spectral simulation were obtained using the Eclipse software provided by VG Scientific. Samples were treated by a reducing mixture ($H_2/N_2$, propane/$N_2$ or ethane/$N_2$ = 20/80) for 30 min at 300 °C in the pre-treatment chamber, and then introduced (without exposure to air) inside the vacuum chamber for acquisition of XPS spectrum (HT-XPS). Then the reduced samples were submitted to $O_2/N_2$ = 20/80 flow for 30 min at 300 °C in the pre-treatment chamber and examined as before. Differential Scanning Calorimetry and ThermoGravimetric Analyses (TGA/DSC) were carried out with a TA-Instrument SDT-2960 thermobalance in flowing $N_2/O_2$ (80:20) or reducing/oxidizing atmosphere up to 400 °C. The temperature rate was 10 °C/min for ~10–15 mg of catalyst.

The oxidation of ethane was carried out in a conventional fixed bed microreactor with on line analysis by gas chromatography. Ethane, oxygen and nitrogen were fed ($C_2H_6/O_2/N_2$ = 40/6/54) and the reactor was operated at 240–300 °C and contact time $\tau$ = 1.2 s for 3 mL of catalyst ($P$ = 1 atm).

## 3. Results and discussion

### 3.1. Influence of Pd and/or Nb on the structural properties of $MoV_{0.4}O_y$ catalyst

For a better comprehension, the main structural characteristics of $MoV_{0.4}$-based catalysts with (or without) Pd and/or Nb are recalled in Table 1 [35,36]. The main influence of Nb on the characteristics of $MoV_{0.4}$ samples consists of (i) a limited number of oxides (XRD) and the nanosize of their particles, (ii) the presence of controlled amount of $V^{4+}$ specie (XPS), and, (iii) the stabilisation of the main mixed-valency oxide which is $Mo_5O_{14}$, probably by insertion of V and of Nb (further called $(MoVNb)_5O_{14}$). This phase was already observed in MoVNbO catalysts [21,22] at variance with other works [7,20,24]. When Pd is added to $MoV_{0.4}$, the particles are not stable under the laser beam (LRS) and their volatilisation is observed. When $MoV_{0.4}Pd_\varepsilon$ is heated in air at 550 °C, XRD shows the patterns of $MoO_3$ and $V_2O_5$. On the contrary the Raman lines characteristic of $Mo_5O_{14}$ as determined by Mestl and co-workers [30,31] remain the same in the presence of both Nb and Pd, besides those of α-$MoO_3$. The promotion of MoVNb by Pd does not strongly modify the structural characteristics of MoVNb (see Table 1). The influence of Pd and/or Nb is even obvious at the precursor stage (after drying). For example, the spectrum of anhydrous ammonium heptamolybdate is only displayed in the case of the particles of MoVNb precursor which are statistically homogeneous at microscale. On the contrary, the particles of MoV and MoVPd precursors are not homogeneous as the spectra reveal the presence of ammonium heptamolybdate and $MoO_3$.

### 3.2. Redox experiments on MoV(NbPd) catalysts

In situ laser Raman spectra of MoV catalyst heated up to 475 °C in reducing atmosphere ($H_2$) show that $MoO_3$ (820, 990 $cm^{-1}$) is reduced above 350 °C to $MoO_2$ which is identified by bands at 230, ~460, ~492 $cm^{-1}$ (Fig. 1). The lines of vanadium suboxides or of $Mo_{0.67}V_{0.33}O_2$ solid solution are not present, at variance with the case of MoVNb(Pd) (vide infra). There is also a broad massif at ca. 830–930 $cm^{-1}$ that may account for the presence of $Mo_5O_{14}$-type oxide and which is better seen on heating at 150 °C. In the case of MoVNbPd, the massif with lines at 928, 872, 830 $cm^{-1}$ is

**Table 1**
Main characteristics of $MoV_{0.4}O_y$ without or with niobium after heat treatment up to 350 °C (after [35,36]) and of MoVNbPd (this work)

| Characteristics | Catalyst without Nb | Catalyst with Nb or Nb + Pd |
|---|---|---|
| Structure (XRD) | α-$MoO_3$, hex-$MoO_3$[a], $Mo_5O_{14}$[a], $V_{0.97}Mo_{0.95}O_5$ | α-$MoO_3$, $Mo_5O_{14}$[a,b] |
| Structure (LRS) | α-$MoO_3$ and $V_2O_5$ | $Mo_5O_{14}$[a,b] (+α-$MoO_3$) |
| Texture (XRD, SEM) | Crystalline | Amorphous (dp[c] ≈50 nm) |
| Surface properties (XPS) | $Mo^{6+}$, $V^{4+}$ + $V^{5+}$ | $Mo^{6+}$, $Nb^{5+}$, $V^{4+}$ + $V^{5+}$. |
| Surface atomic ratio (XPS) | V/Mo < 0.4 | V/Mo ≥ 0.4; Nb/Mo < 0.12 |
| Reactivity observed by laser heating (LRS) | Unstability (volatilisation) | Stabilisation of $Mo_5O_{14}$[a,b] |
| Reactivity (TPR/TPO) | Decomposition accelerated | Stabilisation against oxidation |

[a] May contain V.
[b] May contain Nb.
[c] Mean particle size.

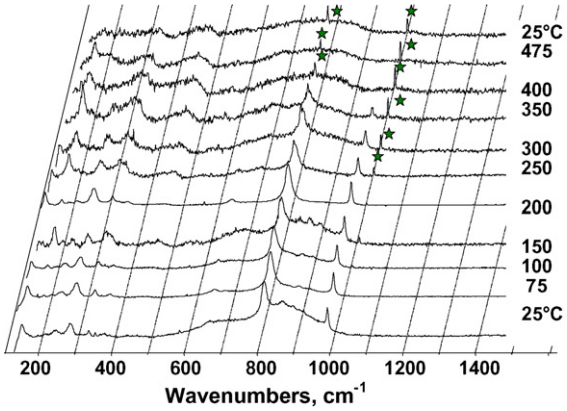


**Fig. 1.** In situ laser Raman spectra of $MoV_{0.4}$ during reduction by $H_2/N_2$ (stars: spikes).

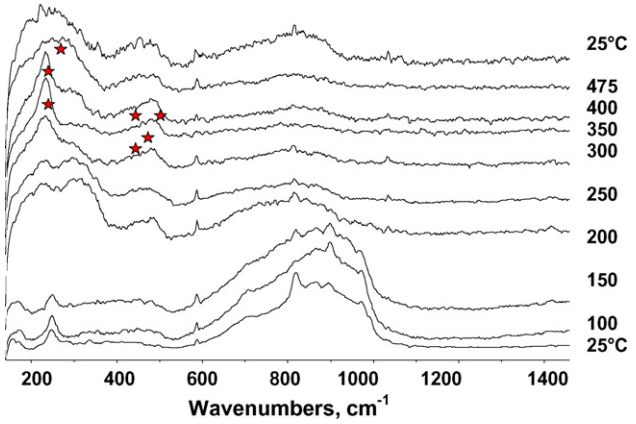


**Fig. 2.** In situ laser Raman spectra of $MoV_{0.4}Nb_{0.12}Pd_{e-4}$ during reduction by $H_2/N_2$ (stars: lines of $MoO_2$).

characteristic of $Mo_5O_{14}$-type oxide (broad massif at ca. 700 $cm^{-1}$ and lines at 940–860 $cm^{-1}$) [30,31]. This pattern vanishes above 200 °C (Fig. 2). $MoO_3$ is also present (line at 820 and shoulder at 980 $cm^{-1}$). After oxidation of MoV and MoVNbPd catalysts in air, the intensity of lines assigned to $Mo_5O_{14}$-type in MoV decreases while that of $MoO_3$ increases irreversibly. In the case of MoVNbPd, the massif of $(MoVNb)_5O_{14}$ is still observed at 475 °C (Fig. 3). Therefore, HT-LRS experiments demonstrate that Nb additive is responsible for the stabilization of $(MoVNb)_5O_{14}$ against (re)oxidation.

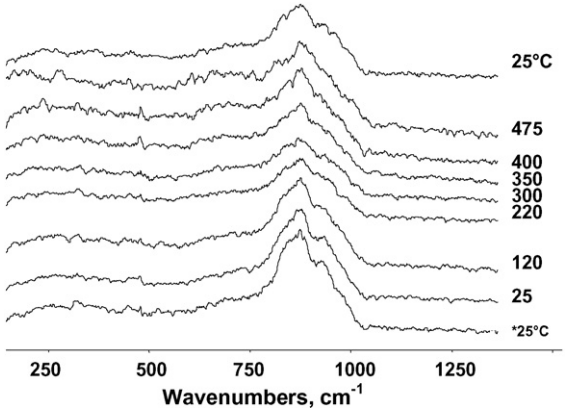


**Fig. 3.** In situ Raman spectra of MoVNbPd heated in air (*: as is).

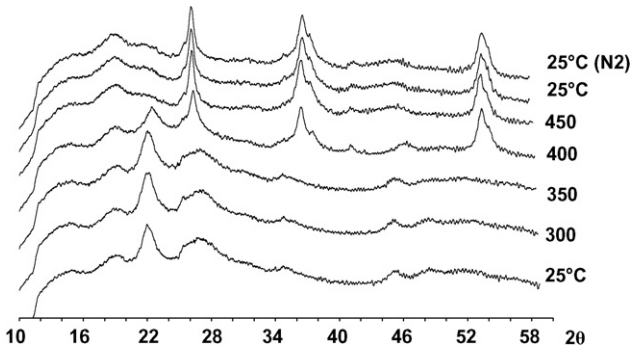


**Fig. 4.** HT-XRD patterns of the reduction of MoVNbPd in $H_2/N_2$.

The oxides which were present in MoV at R.T. (Table 1) are stable up to 350 °C during the in situ reduction in $H_2/N_2$ studied by HT-XRD. Above this temperature, only the characteristic lines of $MoO_2$ appear at $2\theta$ ~26.0, 37.0, 41.5, 53–54° and no line can be assigned to $VO_2$ for Nb-free (MoV and MoVPd) catalysts. In the case of Nb-containing catalysts, the broad pattern accounting for a mixture of nanocrystalline particles of $(MoVNb)_5O_{14}$ and of α-$MoO_3$ [30] remains up to 300 °C. Above 400 °C, the lines $2\theta$ ~22.0° for $(MoVNb)_5O_{14}$ and 27.0° for $MoO_3$ respectively vanish to give rise to lines of $Mo_{0.67}V_{0.33}O_2$ solid solution (Fig. 4). Consequently, this experiment is a proof that vanadium and part of molybdenum were already mixed inside a solid solution, whereas this could not be demonstrated in the absence of Nb. Owing to the broadness of the XRD pattern it cannot be ascertained that Nb is also inserted in the MoV solid solution. However, and although surprisingly no $(Nb,Mo)O_2$ solid solution is known in literature, $Nb^{5+}$ could theoretically enter the lattice of $MoO_2$ because its ionic radius is 0.64 vs. 0.65 Å for $Mo^{4+}$ (both for 6-coordination). After reoxidation of MoVNb in air, the occurrence of several lines ($2\theta$ = 22.0°, 23.2°, 31.4°, 33.3°, 38.5°) assigned to crystalline $(MoVNb)_5O_{14}$ is remarkable. This is at variance with the MoV pattern after reoxidation in which only lines of α-$MoO_3$ are present. Nb is as well responsible for the stabilisation of $(Mo,V,Nb)O_2$ and of $(Mo,V,Nb)_5O_{14}$ without crystallisation of α-$MoO_3$ (and $V_9Mo_6O_{40}$ or $V_2MoO_8$) even after heating in air at 450 °C.

When hydrogen is replaced by ethane in HT-XRD, the observed phenomena are the same. In the presence of Nb the solid solution $V_{0.33}Mo_{0.67}O_2$ is formed by reduction, and after reoxidation at 450 °C $(MoVNb)_5O_{14}$ remains present besides $MoO_3$ and $V_2MoO_8$. The only slight difference is the crystallinity of $(MoVNb)_5O_{14}$ which is less improved after reoxidation following reduction by ethane than it was in the case of reduction by $H_2$.

HT-XPS redox experiments were performed on catalysts after reduction by $H_2$, and after reoxidation in air (both at 300 °C in the pre-treatment chamber). The mean binding energies for all samples before reduction are characteristic of $Mo^{6+}$ ($Mo3d_{5/2}$: 232.2–232.7 eV), $Nb^{5+}$ ($Nb3d_{5/2}$: 206.6–207.0) [37], and of mixed $V^{5+}$–$V^{4+}$. The decomposition of the latter photopeak shows that the $V^{5+}/(V^{5+}+V^{4+})$ atomic ratio decreases along MoVPd > MoVNb, MoVNbPd > MoV series (Table 2). For each catalyst, this ratio decreases during reduction as expected, and its original value is approximately recovered by oxidation. Molybdenum and niobium remain in a high oxidation state (ca. 6+ and 5+, respectively) except in the case of MoVNbPd. Indeed the decomposition of Mo, V, Nb photopeaks shows the presence of three species for Mo and V ($Mo^{6+}/Mo^{5+}/Mo^{4+}$ = 1.23:1:0.94; $V^{5+}/V^{4+}/V^{3+}$ = 0.43:1:0.82), as well as of some $Nb^{4+}$ ($Nb^{5+}/Nb^{4+}$ = 0.33) (Fig. 5). For a given catalyst, the V/Mo surface atomic ratio does not change much during reduction and reoxidation. However it increases along MoV, MoVPd (0.25–0.27) < MoVNb (0.28–0.33) < MoVNbPd (0.36–

**Table 2**
Experimental atomic ratios of MoV(NbPd) catalysts during redox experiments

| | MoV | | MoVPd | | MoVNb | | | MoVNbPd | | |
|---|---|---|---|---|---|---|---|---|---|---|
| | V/Mo | $V^{5+}/V_{tot}$ | V/Mo | $V^{5+}/V_{tot}$ | V/Mo | Nb/Mo | $V^{5+}/V_{tot}$ | V/Mo | Nb/Mo | $V^{5+}/V_{tot}$ |
| R.T. | 0.26 | 0.73 | 0.27 | 0.89 | 0.31 | 0.11 | 0.81 | 0.39 | 0.06 | 0.80 |
| Reduction | 0.26 | 0.35 | 0.25 | 0.24 | 0.28 | 0.14 | 0.36 | 0.37 | 0.04 | 0.16 |
| Reoxidation | 0.26 | 0.62 | 0.26 | 0.62 | 0.33 | 0.16 | 0.73 | 0.36 | 0.03 | 0.67 |

$V_{tot} = V^{5+} + V^{4+}$.

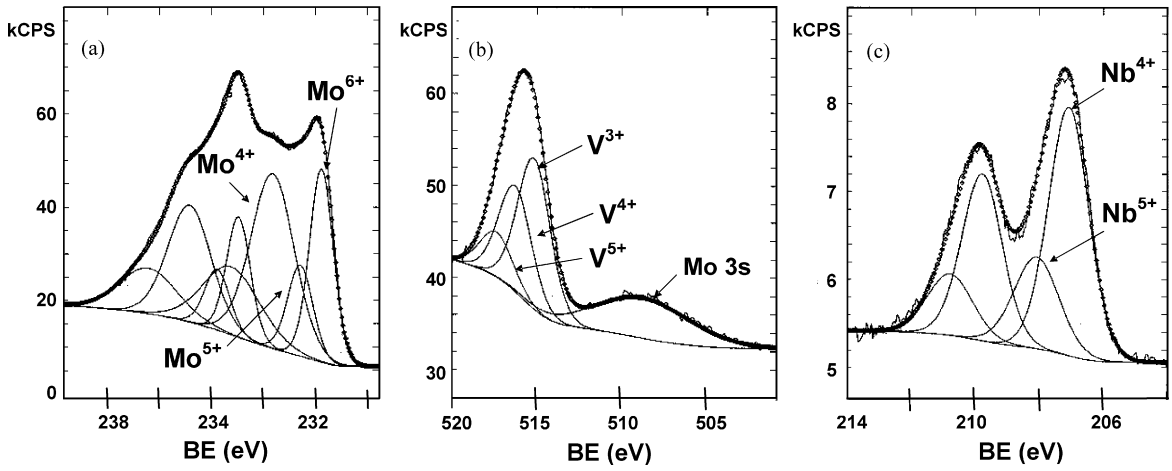


**Fig. 5.** Decomposition of XPS spectrum of MoVNbPd after reduction by $H_2/N_2$; (a) Mo$3d_{5/2}$, (b) V$2p_{3/2}$ and (c) Nb$3d_{5/2}$ photopeaks.

0.39). The difference between Nb-free and Nb-containing catalysts is again put in evidence: the surface of the latter is slightly enriched with vanadium as compared with the former. In the presence of Pd, less Nb is present close to the surface (Nb/Mo ~0.05). The difference between MoVNb and MoVNbPd could therefore be due to Pd hindering too many Nb atoms to occur on the surface. When hydrogen was replaced by propane at 400 °C, little change of atomic ratios was observed. On the whole, the $V^{5+}/V_{tot}$ ratios were greater and the Mo (and Nb) oxidation state in MoVNbPd remained ca. 6+ (5+, respectively). This behaviour was expected from experiments with propane which is a milder reducing agent than hydrogen.

The transformation of catalysts during heating in air was studied by TGA/DSC to see if any reoxidation of the $V^{4+}$ (or $Mo^{5+}$) specie detected by XPS proceeds. There is no significant gain of weight up to 500 °C. The main event is a small exothermic signal at ~410 °C for MoV which is assigned to the transformation of metastable hexagonal h-$MoO_3$ into orthorhombic α-$MoO_3$. A similar exotherm is observed at higher temperature (~480 °C) for MoVNbPd, and is assigned to the transformation of the h-$V_{0.12}Mo_{0.88}O_{2.94}$ solid solution isostructural to h-$MoO_3$ into α-$V_{0.12}Mo_{0.88}O_{2.94}$ solid solution isostructural to α-$MoO_3$ as studied by Dupont et al. [38]. This observation is in agreement with previous results obtained by XRD during heating in $O_2$ [36]. The fact that this transformation occurs in MoVNbPd at a higher temperature than in MoV confirms the role of Nb in favoring the incorporation of V in Mo oxide(s) and in stabilizing the hexagonal vs. orthorhombic structure. The framework of h-$MoO_3$ consists of rings of pairs of edge-sharing Mo(V) octahedra linked by corners, which are stabilized by $NH_4^+$, $H^+$ and/or alkaline cations. This open structure is more prone to accept foreign cations (V, Nb) than is the more stable structure of α-$MoO_3$, and very probably it also favors the formation of tunnel structures like $Mo_5O_{14}$.

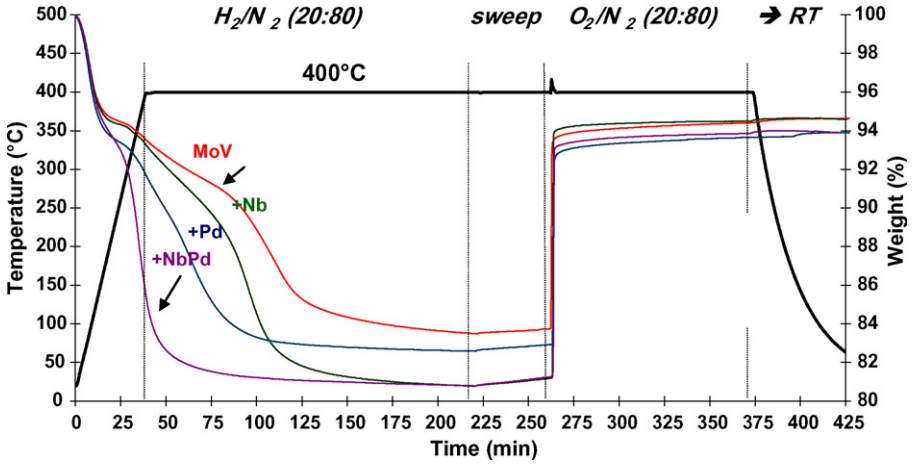


**Fig. 6.** TGA of MoV, MoVNb, MoVPd and MoVNbPd in reducing ($H_2/N_2$) and oxidizing (air) conditions at 400 °C.

The TGA of MoV, MoVNb, MoVPd and MoVNbP catalysts during reduction by $H_2/N_2$ = 20/80 at 400 °C followed by reoxidation in air (400 °C) is presented in Fig. 6. After the loss of adsorbed water, the reduction proceeds at different rates depending on the composition, whereas the reoxidation is fast (approximately 100 times faster than reduction), the final state being close to the one once the sample was dehydrated. According to their known chemical reactivity, the ultimate phases after reduction should be $MoO_2$, $VO_2$ or $V_2O_3$ and $NbO_2$, some of them being already characterized by HT-XRD in $H_2$. The rate of reduction increases upon addition of Pd to MoV (6–16.$10^{-2}$ wt%/min), and to MoVNb (10–35.$10^{-2}$ wt%/min), but there is little variation of $\Delta m/m$ as expected owing to the very small amount of Pd. Upon addition of 0.12Nb to $MoV_{0.4}$, the slope of reduction increases to a less extent (6–10.$10^{-2}$ wt%/min) and the deepness of reduction increases. The values of $\Delta m/m$ account approximately for the reduction of $Mo^{6+}$, $V^{5+}$, $Nb^{5+}$ to $Mo^{4+}$, $V^{3+}$ and $Nb^{4+}$, respectively. Therefore, TGA experiments demonstrate that Pd and/or Nb do have an influence on the redox system. The samples were analysed by XRD after the reoxidation step. In the cases of Nb-containing samples (MoVNb and MoVNbPd), lines of crystalline $(MoVNb)_5O_{14}$ could be identified (besides $MoO_3$), whereas a mixture of $MoO_3$, $V_9Mo_6O_{40}$ or $V_2MoO_8$ ($2\theta$ = 18.2° and 21.8°) and $V_{0.95}Mo_{0.97}O_5$ was obtained in Nb-free samples.

The same experiments performed with propane or with ethane instead of $H_2$ show that the reduction, which begins at lower temperature, is slowed down and that the loss of weight is smaller. The reoxidation is again faster than the reduction. However the influence of Pd may be different because it does not increase the rate of reduction of MoV, contrary to experiments with hydrogen. Palladium (II) may be still present during reduction by propane or ethane, whereas it was probably metallic ($Pd^0$) during reduction in $H_2$ (if present, PdO is easily reduced). These experiments show that the reduction of all samples can be regarded as 'reversible', whatever the reducing gas (hydrogen, propane or ethane), because the initial weight (after loss of water) is recovered by reoxidation in air. However the oxides identified before and after reoxidation differ in the case of Nb-free samples, whereas in the presence of when Nb the same $(MoVNb)_5O_{14}$ oxide is present.

### 3.3. Attempts to correlate structural properties with catalysis

In Table 3 are gathered the values of the conversion of ethane and yields in acetic acid and ethylene obtained at 260 °C. It was shown earlier [36,37] that in the chosen operating conditions the temperature could not be increased above 280 °C while maintaining the conversion of oxygen less than 100%. These figures should be compared at the same conversion but this is not possible in the used range of temperature, because with MoVPd the conversion reaches a maximum close to 3% [36]. The ratio of yields $R = Y_{AA}/Y_{C_2H_4}$ used as a "measure" of selectivity increases along MoV (0.31) ≈ MoVNb (0.33) < MoVPd (0.81) < MoVNbPd (1.04), and at a similar conversion (6–6.5%) the yield of acetic acid with MoVNbPd is 2.5 times that obtained with MoVNb. Therefore, the influence of the composition of the catalyst on the formation of acetic acid or ethylene is noticeable and worthwhile to discuss. Although the catalysts here studied are not "equilibrated" as they should be in industrial conditions, it is necessary to recall that at the low temperature of reaction chosen, the structural modifications of the bulk of the catalyst are hardly processing.

**Table 3**
Conversion of ethane $X_{C_2H_6}$, yields of acetic acid ($Y_{AA}$) and of ethylene ($Y_{C_2H_4}$), and ratio of yields $R = Y_{AA}/Y_{C_2H_4}$ during the catalytic oxidation of ethane on MoV-based catalysts at 260 °C (unless specified)

| | MoV | MoVPd | MoVNb | MoVNb* | MoVNbPd |
|---|---|---|---|---|---|
| $X_{C_2H_6}$ | 5.1 | 4.4 | 9.5 | 6.5 | 6.0 |
| $Y_{AA}$ | 1.1 | 1.7 | 2.2 | 1.8 | 2.7 |
| $Y_{C_2H_4}$ | 3.5 | 2.1 | 6.7 | 4.5 | 2.6 |
| $R$ | 0.31 | 0.81 | 0.33 | 0.41 | 1.04 |

Complementary yields: $CO_x$; * reaction at 220 °C.

The addition of 0.12 Nb to $MoV_{0.4}$ leads to a nearly two-fold increase of the conversion of ethane $X_{C_2H_6}$ and of the yields of acetic acid (AA) and ethylene (Table 3). The structural characterization just detailed above shows that upon addition of Nb, (i) the incorporation of V in Mo oxides is facilitated, (ii) nanoparticles of $(MoVNb)_5O_{14}$ and $MoO_3$ prevail (XRD and LRS), (iii) $(MoVNb)_5O_{14}$ is quite stable against reoxidation (in situ LRS), and (iv) it is more crystalline after reduction (HT-XRD). Moreover, MoVNb is more easily reducible than MoV (TGA). The higher conversion of ethane on MoVNb compared with MoV is certainly related to the nanosized particles of the former (as shown by the quite amorphous XRD pattern). The ratio of yields $R = Y_{AA}/Y_{C_2H_4}$ is roughly the same, which means that, in first approximation, the same sites are present on the surface. If α-$MoO_3$ is considered at the very best as inactive, the surface vanadium specie would be responsible for selectivity when stabilized as $V_{0.12}Mo_{0.88}O_{2.94}$ and/or $(MoVNb)_5O_{14}$.

Compared to Nb, the addition of a very small amount of Pd to MoV or to MoVNb does not lead to obvious structural differences. However in both cases the reactivity is strongly enhanced as shown by the reduction which proceeds faster (TGA). Doping MoV by Pd leads to unstable particles when heated by laser (LRS), and the mean oxidation state of surface V specie ($V^{5+}/V_{tot}$) is higher by 20% while the V/Mo ratio does not change much (XPS). When niobium is present, the particles are stable (laser heating), the mean oxidation state of surface V specie is similar, but V/Mo increases (XPS) for MoVNbPd vs. MoVNb (and others). The formation of acetic acid is enhanced by Pd as shown by $R$ values (0.31–0.81 for MoV and 0.33–1.04 for MoVNb) (Table 3), but the yield of $CO_x$ is very high on MoVPd (and very low on MoVNbPd). That is to say that the effect of Pd depends on the presence of Nb, and in turn on the formation of $(MoVNb)_5O_{14}$. The results suggest that if Pd is not stabilized by an oxidic matrix, it may easily be reduced to $Pd^0$ and that in such a case it acts as a catalyst of complete oxidation of ethane and intermediates. If it is stabilized, its role in catalysis could be to promote the transformation of ethylene to acetic acid. This explanation has been proposed by Baerns and co-workers [28], and it stems from a study by Montarnal and co-workers [39] in which $V_2O_5$ doped with Pd has been shown to oxidize ethylene to acetic acid.

## 4. Conclusion

The structural properties of $MoV_{0.4}$ samples differing by the presence or not of Nb, Pd, have been studied by in situ methods by varying temperatures and reducing and/or oxidizing atmospheres. All experiments show that the role of Nb is prominent. Nb stabilizes the $Mo_5O_{14}$-type oxide (besides α-$MoO_3$ or α-$V_{0.12}Mo_{0.88}O_{2.94}$), probably because it enters the lattice together with vanadium. Nb is as well responsible for the nanosize of the particles, which in turns behave as more active catalysts in the oxidation of ethane. This $(MoVNb)_5O_{14}$ phase is stable against oxidation up to 450 °C, as well as during reduction by ethane or propane. By reduction in $H_2$ it gives rise to $(VNb)_xMo_{1-x}O_2$ suboxide which is reoxidized to $V_{0.12}Mo_{0.88}O_{2.94}$ and other mixed V, Mo oxides. Palladium fastens the reduction step, as also observed by XPS with $H_2$ pre-treatment. However its role is different according to the absence of Nb, in which case it favors the unstability of the catalyst (LRS), or to its presence, in which case the

selectivity to acetic acid increases. The stability and location of Pd onto the surface are questionable. As metallic $Pd^0$, if it is simply dispersed as it would be on classical supports like alumina, it would be responsible for combustion. It may be the case of MoVPd during catalysis, because carbon oxides amount up to a quarter or the products, but not on the other catalysts [35,36]. But if it remains as $Pd^{2+}$ it could be located and therefore stabilized in the tunnels of the $Mo_5O_{14}$ structure. Simple calculations by the bond valence theory applied in inorganic chemistry [40] show indeed that $Pd^{2+}$ could keep its usual square coordination if it was located in the hexagonal or pentagonal tunnels.

## Acknowledgements

L. Burylo, O. Gardolle, L. Gengembre, M. Frère, C. Dujardin, A.-S. Mamède are thanked for HT-XRD, TGA/DSC experiments, XPS and in situ LRS, respectively. O. Mentré is acknowledged for calculations with the valence bond theory, and M. Roussel is indebted to SABIC for a post-doctoral position and permission to publish this work.

## References

[1] S. Albonetti, F. Cavani, F. Trifirò, Catal. Rev. Sci. Eng. 38 (1996) 414.
[2] F. Cavani, F. Trifirò, P. Arpentinier, The Catalytic Technology of Oxidation, Technip, Paris, 2001.
[3] K. Karim, M. Al-Hazmi, A. Khan, US6060421, 2000, to SABIC.
[4] K. Karim, B.Y. Subrai, N.F. Bin, Z.S. Irshad, US6114278, 2000, to SABIC.
[5] E. Bordes, Stud. Surf. Sci. Catal. 67 (1991) 21.
[6] E. Bordes, in: R.W. Joyner, R.A. van Santen (Eds.), Elementary Reaction Steps in Heterogeneous Catalysis, Kluwer Acad. Publ., 1993, pp. 137–153.
[7] E.M. Thorsteinson, T.P. Wilson, F.G. Young, P.H. Kasai, J. Catal. 52 (1978) 116.
[8] L. Tessier, E. Bordes, M. Gubelmann-Bonneau, Catal. Today 24 (1995) 335.
[9] M. Roy, M. Gubelmann-Bonneau, H. Ponceblanc, J.C. Volta, Catal. Lett. 42 (1996) 93.
[10] E. Bordes, M. Gubelman-Bonneau, L. Tessier, French Patent 2720063, 1995, to Rhône-Poulenc Chimie; US Patent 6,114,274, 2000, to Rhône-Poulenc Chimie).
[11] D.I. Enache, E. Bordes-Richard, A. Ensuque, F. Bozon-Verduraz, Appl. Catal. A: General 278 (2004) 93;
D.I. Enache, E. Bordes-Richard, A. Ensuque, F. Bozon-Verduraz, Appl. Catal. A: General 278 (2004) 103.
[12] S. Wajki, Y. Koyasu, H. Nakamura, T. Ushikubo, EP0608838, 1994, to Mitsubishi Kasei Corporation.
[13] T. Ushikubo, K. Oshima, A. Kayou, M. Hatano, Stud. Surf. Sci. Catal. 112 (1997) 473.
[14] H. Hibst, L. Marosi, A. Tenten, US5807531, 1998, to BASF.
[15] M. Aouine, J.L. Dubois, J.M.M. Millet, Chem. Commun. (2001) 1180.
[16] D. Vitry, Y. Morikawa, J.L. Dubois, W. Ueda, Appl. Catal. A: General 251 (2003) 411.
[17] J.M.M. Millet, H. Roussel, A. Pigamo, J.L. Dubois, J.C. Dumas, Appl. Catal. A: General 232 (2003) 77.
[18] R.K. Grasselli, J.D. Burrington, D.J. Buttrey, P. De Santo Jr., C.G. Lugmair, A.F. Volpe, T. Weing, Topics Catal. 23 (2003) 23.
[19] P. De Santo Jr., D.J. Buttrey, R.K. Grasselli, C.G. Lugmair, A.F. Volpe, B.H. Toby, T. Vogt, Z. Krist. 219 (2004) 152.
[20] R. Burch, R. Swarnakar, Appl. Catal. 70 (1991) 129.
[21] M. Merzouki, E. Bordes, B. Taouk, L. Monceaux, P. Courtine, Stud. Surf. Sci. Catal. 72 (1992) 81.
[22] M. Merzouki, B. Taouk, L. Tessier, E. Bordes, P. Courtine, New frontiers in catalysis, in: L. Guczi, F. Solymosi, P. Tétényi (Eds.),10th Int. Cong. Catalysis, Budapest, Hungary, July 20–25, 1992, Stud. Surf. Sci. Catal. 75 (1993) 753.
[23] P. Courtine, E. Bordes, Appl. Catal. A: General 157 (1997) 45.
[24] K. Ruth, R. Kieffer, R. Burch, J. Catal. 175 (1998) 13;
K. Ruth, R. Kieffer, R. Burch, J. Catal. 175 (1998) 27.
[25] J.M. López Nieto, P. Botella, M.I. Vásquez, A. Dejoz, Chem. Commun. (2002) 1906.
[26] D. Linke, D. Wolf, M. Baerns, O. Timpe, R. Schlögl, S. Zeyß, U. Dingerdissen, J. Catal. 205 (2002) 16.
[27] W. Ueda, K. Oshihara, Appl. Catal. A: General 200 (2000) 135.
[28] D. Linke, D. Wolf, M. Baerns, S. Zeyß, U. Dingerdissen, J. Catal. 205 (2002) 32.
[29] H. Vogel, R. Böhling, H. Hibst, Catal. Lett. 62 (1999) 71.
[30] M. Dieterle, G. Mestl, J. Jäger, Y. Uchida, H. Hibst, R. Schlögl, J. Mol. Catal. A: Chem. 174 (2001) 169.
[31] G. Mestl, J. Raman Spectrosc. 33 (2002) 333.
[32] H. Werner, O. Timpe, D. Herein, Y. Uchida, N. Pfänder, U. Wild, R. Schlögl, Catal. Lett. 44 (1997) 153.
[33] P. Moriceau, A. Lebouteiller, E. Bordes, P. Courtine, Phys. Chem. Chem. Phys. 1 (1999) 5735–5744;
P. Moriceau, B. Taouk, E. Bordes, P. Courtine, Catal. Today 61 (2000) 197–201;
P. Moriceau, B. Taouk, E. Bordes, P. Courtine, Stud. Surf. Sci. Catal. 130 (2000) 1811.
[34] E. Bordes-Richard, P. Courtine, in: J.L.J. Fierro (Ed.), Metal Oxides: Chemistry and Applications, Marcel Dekker, 2005, pp. 319–352.
[35] M. Roussel, M. Bouchard, E. Bordes-Richard, K. Karim, S. Al-Sayari, Catal. Today 99 (2005) 77.
[36] M. Roussel, M. Bouchard, E. Bordes-Richard, K. Karim, S. Al-Sayari, Appl. Catal. A: General 308 (2006) 62.
[37] http://www.lasurface.com/.
[38] L. Dupont, D. Larcher, F. Portemer, M. Figlarz, J. Solid State Chem. 121 (1996) 339.
[39] J.L. Seoane, P. Boutry, R. Montarnal, J. Catal. 63 (1980) 191;
J.L. Seoane, P. Boutry, R. Montarnal, J. Catal. 63 (1980) 202.
[40] I.D. Brown, Comput. Modell. Inorg. Crystallog. (1997) 23.